Laurentide Ice Sheet persistence during Pleistocene interglacials

- 2 Danielle E. LeBlanc¹; Jeremy D. Shakun¹; Lee B. Corbett²; Paul R. Bierman²; Marc W. Caffee ³;
- 3 Alan J. Hidy⁴
- 5 USA
- 6 ² Rubenstein School of the Environment and Natural Resources, University of Vermont,
- 7 Burlington, VT 05405, USA
- 8 ³ Department of Physics and Astronomy and Department of Earth, Atmospheric, and Planetary
- 9 Sciences, Purdue University, West Lafayette, IN 46202, USA
- 10 ⁴ Center for Accelerator Mass Spectrometry, Lawrence Livermore National Laboratory,
- 11 Livermore, CA 94550, USA

12 ABSTRACT

- While there are no ice sheets in the Northern Hemisphere outside of Greenland today, it is
- uncertain whether this was also the case during most other Quaternary interglacials. Here, we
- show, using in situ cosmogenic nuclides in ice-rafted debris, that the Laurentide Ice Sheet was
- 16 likely more persistent during Quaternary interglacials than often thought. Low ²⁶Al/¹⁰Be ratios
- 17 (indicative of burial of the source area) in marine core sediment suggest sediment source areas
- experienced only brief (on the order of kyr) and/or infrequent ice-free interglacials over the last
- million years. These results imply that complete Laurentide deglaciation may have only occurred
- when climate forcings reached levels comparable to those of the early Holocene, making our
- 21 current interglacial unusual relative to others of the mid-to-late Pleistocene.

22 **INTRODUCTION**

Since the start of the Pleistocene epoch (~2.6 Ma), continental ice sheets have ebbed and flowed over glacial-interglacial cycles across North Atlantic landscapes. A longstanding question is to what extent past interglacials were like today. Did Northern Hemisphere ice sheets outside Greenland always disappear such as in the Holocene, or did remnant ice domes survive during interglacials? The former scenario would suggest a low deglaciation threshold where the conditions required for ice disappearance were reached during most or all Pleistocene interglacials. The latter scenario would suggest that ice sheets only fully disappear when multiple factors conspire for long enough to drive complete deglaciation (Ullman et al., 2015).

Understanding the history of the Laurentide Ice Sheet is of particular interest as it was the last Northern Hemisphere ice sheet to deglaciate during the Holocene and is key to determining whether past interglacials reached ice-free conditions outside of Greenland. Reconstructing Laurentide margins prior to the Last Glacial Maximum is difficult due to the limitations of traditional geologic records. Terrestrial records are discontinuous due to their removal by glacial erosion. Benthic δ^{18} O provides a continuous record of ice volume changes (Lisiecki and Raymo, 2005), but is difficult to link to a specific ice sheet; the isotope signal is also confounded by an uncertain ocean temperature component and may not be a reliable recorder of ice volume (Dalton et al., 2022). The presence of ice-rafted debris in marine sediments indicates times with large, marine-terminating ice sheets, but ice-rafted debris cannot constrain the extent of retreat when ice margins fall short of coastlines. Given these limitations, reconstructions of Laurentide margins during Pleistocene interglacials have only been produced for the last interglacial and have large ranges from no ice to sizable ice domes spanning much of Canada (Fig. 1) (Kleman et al., 2010; Batchelor et al., 2019; Miller et al., 2022).

METHODS

Here, we assess Laurentide Ice Sheet persistence during past interglacials by measuring concentrations of cosmogenic ¹⁰Be and ²⁶Al in quartz sand across North Atlantic Heinrich layers (layers rich in ice-rafted debris from Laurentide discharge episodes during the last glacial period). Cosmogenic nuclides in ice-rafted debris record an integrated exposure, burial, and erosion history of the regions from which sediment was sourced. During ice-free times, nuclides accumulate in quartz within rock and sediment exposed to cosmic radiation. Nuclide production via spallation reactions is highest at the surface (~4 atoms g⁻¹ yr⁻¹ at high latitudes near sea level) and rapidly attenuates with depth, but low levels of production (<10⁻¹ atoms g⁻¹ yr⁻¹) by muons extend several tens of meters into the subsurface (Gosse and Phillips, 2001).

During times of significant ice sheet cover, most nuclide production halts because surface materials are shielded from cosmic rays. Because 26 Al ($t_{1/2}$ = 0.7 Myr) decays more rapidly than 10 Be ($t_{1/2}$ = 1.4 Myr), the 26 Al/ 10 Be ratio decreases below the production value during intervals of burial longer than $\sim 10^5$ years. The long half-lives of 10 Be and 26 Al, and their accumulation far into the subsurface by muonic production, means they are well suited to retain a memory of near-surface process history over Pleistocene time scales, even in areas with deep erosion (Briner et al., 2016).

Glacial erosion removes heavily irradiated material from the surface and exhumes progressively nuclide-poorer material at depth. Glacial sediment is derived primarily from warmbased, erosive sectors of an ice sheet; thus, cosmogenic nuclide data provide information about ice sheet behavior in sediment-generating regions. Although the ice-rafted debris we analyzed was transported to the ocean by marine-terminating ice during the last glacial period, cosmogenic nuclides in ice-rafted debris reflect prior exposure, burial, and erosion in the sediment source areas.

We made 26 paired cosmogenic nuclide measurements from Heinrich layers 1 through 6 (H1-6, 17-60 ka) as well as intervening layers at core sites on the west and east sides of the North Atlantic (Fig. 1). To obtain enough quartz sand for measurement (> 5 g), multiple subsamples were amalgamated from each layer. Western core sites (IODP Sites U1302 and U1303 at 50.2°N, 45.6°W and 50.2°N, 45.7°W and EW93-02 JPC-02 at 48.8°N, 45.1°W) sit at the mouth of the Labrador Sea and received icebergs predominantly from eastern Canada via the Labrador Current (Mao et al., 2014; Fendrock et al., 2022). Eastern core sites (BOFS-5K at 50.7°N, 21.9°W and DSDP Site 609 at 49.9°N, 24.2°W and IODP Site U1308, a reoccupation of Site 609) lie just east of the Mid-Atlantic Ridge within the last-glacial ice-rafted debris belt (Ruddiman, 1977) at the confluence of iceberg pathways from the Laurentide, Greenland, and European ice sheets (Grousset et al., 1993; Bond and Lotti, 1995; Bigg et al., 2011). All Heinrich layers on the western side of the basin and H1, H2, H4, and H5 in the east contain detrital carbonate, which has been traced to the Hudson Strait sector of the Laurentide Ice Sheet (Hemming, 2004). Because we analyzed quartz rather than carbonate, samples from these Heinrich layers came largely from surrounding silicate terranes up-flow of the Hudson Strait ice stream, which drained a large portion of the Laurentide. Previous provenance work supports this interpretation and shows Heinrich layers contain predominantly Paleoproterozoicaged grains with some younger and older grains, suggesting sediments came from large sectors of northeastern Canada and perhaps Greenland (Hemming et al., 1998; Hemming and Hajdas, 2003). Conversely, intervening layers have a greater number of younger and older grains, especially in eastern North Atlantic samples, indicating contribution from additional sources such as southeastern Canada in the west and Europe in the east during non-Heinrich times (see Supplemental Material).

69

70

71

72

73

74

75

76

77

78

79

80

81

82

83

84

85

86

87

88

89

90

RESULTS

¹⁰Be concentrations decrease through time in western samples but are variable in eastern samples, which we attribute to differences in sediment provenance. The smooth decline in ¹⁰Be concentrations of western samples over time, across both Heinrich and non-Heinrich intervals, is consistent with sediment supplied by erosion and excavation under a single, persistent ice sheet sector, which we infer was part of the Laurentide. Western sample ¹⁰Be concentrations are low, ∼7,000 to 19,000 atoms g⁻¹, less than half the value expected from 10 kyr of interglacial surface exposure (∼40,000 atoms g⁻¹). Such low concentrations imply that sediment with the highest nuclide concentration following last interglacial exposure was removed by erosion earlier in the glacial period and that the ice-rafted debris we measured was sourced primarily from areas of deep subglacial erosion.

We attribute the generally higher, more variable ¹⁰Be concentrations in eastern samples to a mixture of sources, which agrees well with earlier provenance work (see Supplemental Material). During H1, H2, H4, and H5, ¹⁰Be concentrations in the east are indistinguishable from those in the west, suggesting Laurentide-derived icebergs (and the sediments they carried) were distributed across the North Atlantic. ¹⁰Be concentrations are higher in H3 and H6 in the east relative to the west and similar to concentrations in eastern background intervals (times between Heinrich events). These patterns suggest that Laurentide iceberg discharges were smaller during H3 and H6, carried less ice-rafted debris, and/or melted before reaching the east (Bond et al., 1992; Gwiazda et al., 1996).

²⁶Al/¹⁰Be ratios (3.4 to 5.9) are substantially below the high-latitude surface production ratio (~7.3) in all samples, indicating the ice-rafted debris records lengthy Pleistocene histories

dominated by burial (Fig. 2a). Laurentide-derived samples (all western samples and samples H1, H2, H4, and H5 in the east) have a mean ratio of 4.7, which requires a minimum of 900 kyr of decay following initial exposure, assuming the sand we analyzed experienced a single exposure event followed by burial. If the sediment experienced multiple alternating episodes of exposure and burial, the total burial time must be even longer because re-exposure would generate new nuclides at the production value, raising ²⁶Al/¹⁰Be ratios.

DISCUSSION

The lengthy intervals of sediment burial suggested by our data are explained by persistent Laurentide cover in sediment source areas during most of the last million years. Till could shield bedrock from cosmic radiation, but till only partially covers glaciated regions in North America today (Pelletier et al., 2016). Even if till was present, it too would have been irradiated during ice-free interglacials and then exported when ice readvanced. Alternatively, the sediment we analyzed could have been stored underwater in Hudson Bay and Hudson Strait or on continental shelves for many glacial cycles. However, our samples are derived from quartz-bearing terranes which are mostly above sea level, while carbonate sediment in Heinrich layers was derived from submerged carbonate outcrops in Hudson Strait and Hudson Bay. Furthermore, the smoothly decreasing trend in ¹⁰Be concentrations in western samples suggests that the sediments we analyzed came from steadily eroding areas and was not extensively mixed and remobilized during transport to the seafloor.

Forward modeling helps quantify the amount of mid-to-late Pleistocene exposure our data can accommodate and strongly suggests Laurentide ice remained over sediment source areas during most interglacials of the past million years. This model (see the Supplemental Materials) simulates cosmogenic nuclide production in a bedrock profile over the Pleistocene when ice

cover is absent; when ice cover is present, production stops and erosion begins. Nuclides decay continuously with and without ice cover. We run several ice cover histories with different interglacial exposure durations and glacial erosion rates to help bound plausible geologic scenarios. For instance, exposure during every Pleistocene interglacial could have only been on the order of 1-2 kyr, otherwise measured ²⁶Al/¹⁰Be ratios would be closer to the production ratio (Fig. 3, scenario 1). Similar results are found when we limit exposure during the past million years to only Marine Isotope Stage 5e, 9, and 11 (Fig. 3, scenario 2). The data could accommodate longer exposures (~5-10 kyr) during these few mid-to-late Pleistocene interglacials if there was greater exposure during the early Pleistocene and much of the sediment came from very slowly eroding areas where old nuclides were preserved (Fig. 3, scenario 3).

Given the likelihood of sediment mixing, these scenarios represent conservative estimates of ice cover. If our samples are mixtures of sediment from areas with different ice cover histories, some regions would have even lower 26 Al/ 10 Be ratios, and thus more persistent ice cover, than assumed in our modeling. 26 Al/ 10 Be ratios are more heavily influenced by sediments with higher nuclide concentrations because they contribute more nuclides on a per mass basis. This effect helps offset the bias of the sediment record toward the most erosive areas such that the 26 Al/ 10 Be record is more broadly representative of all sediment source regions.

Other lines of evidence are consistent with persistent Laurentide ice during most interglacials. Interglacial sea levels prior to the last interglacial typically fall within 0 ± 20 m relative to the present (Past Interglacials Working Group of PAGES, 2016) and remnant ice existed across parts of northeastern Canada (Dalton et al., 2020) in the early Holocene when sea levels were only 10 to 20 meters below present (Lambeck et al., 2014). Therefore, the lower end

of the 0 ± 20 m interglacial sea level range would be consistent with the survival of some Laurentide sectors during interglacial periods. The frequent occurrence of North Atlantic icerafted debris within mid-to-late Pleistocene interglacials indicates the presence of marine-terminating ice around the North Atlantic even during warm times; ice-rafted debris is rarely absent from cores in the path of Laurentide icebergs near eastern Canada via the Labrador Current and south of Iceland via the North Atlantic Current during the past 750 and 1,700 kyr, respectively (McManus et al., 1999; Channell et al., 2012; Barker et al., 2022). Some of the icerafted debris peaks along eastern Canada also contain detrital carbonate suggesting contribution from the Laurentide (Channell et al., 2012). Although marine δ^{18} O provides a less direct constraint on global ice volume, interglacials in the LR04 δ^{18} O stack reach Holocene levels only a few times during the past two million years (Fig. 3A).

Our data support previous findings of low ²⁶Al/¹⁰Be ratios in material from northeastern Canada. Many cosmogenic nuclide measurements of bedrock from Baffin Island and Labrador have low ²⁶Al/¹⁰Be ratios similar to our results (Fig. 1), indicating long burial and minimal exposure in some locations underlying the Laurentide Ice Sheet over the last million years (e.g. Miller et al., 2006; Briner et al., 2006, 2014; Corbett et al., 2016). Our ice-rafted debris record provides a more spatially-integrated estimate of exposure and erosion history, suggesting larger areas of northeastern Canada than just the specific landscapes previously studied were covered by persistent ice through much of the later Pleistocene, although uncertainties in provenance make it difficult to clearly define the scale of ice cover.

Our data suggest the Laurentide Ice Sheet fully deglaciated only when numerous factors aligned to drive negative surface mass balance for long enough (Ullman et al., 2015). Forcings vary among interglacials, such as the phasing of obliquity and precession, greenhouse gas

184 concentrations, and preceding ice sheet geometry; perhaps only those interglacials with CO₂ 185 maxima near or above Holocene levels reached the threshold for complete deglaciation. Rather 186 than being prototypical, the interglacial that we find ourselves in, with little Northern 187 Hemisphere ice outside of Greenland, may be one of few so extreme in the past million years. 188 ACKNOWLEDGMENTS 189 We thank the IODP Bremen Core Repository, WHOI Seafloor Samples Laboratory, and 190 BOSCORF for sediment samples. David Hodell, Richard Alley, Tamara Pico, Colin Meyer, Alex 191 Robel, Shaun Marcott, and Luke Zoet provided useful conversations. This research was funded 192 by NSF grants ANS-2116208, ANS-2116209 and ANS-2116210, a PRIME Lab seed grant, and 193 Boston College. Prepared in part by LLNL under Contract DE-AC52-07NA27344; LLNL-194 JRNL-832456. 195 REFERENCES CITED 196 Barker, S. et al., 2022, Persistent influence of precession on northern ice sheet variability since 197 the early Pleistocene: Science, v. 376, p. 961–967, 198 https://www.science.org/doi/abs/10.1126/science.abm4033. 199 Batchelor, C.L., Margold, M., Krapp, M., Murton, D.K., Dalton, A.S., Gibbard, P.L., Stokes, 200 C.R., Murton, J.B., and Manica, A., 2019, The configuration of Northern Hemisphere ice 201 sheets through the Quaternary: Nature Communications, v. 10, p. 1–10, 202 doi:10.1038/s41467-019-11601-2. 203 Bigg, G.R., Levine, R.C., and Green, C.L., 2011, Modelling abrupt glacial North Atlantic 204 freshening: Rates of change and their implications for Heinrich events: Global and

Planetary Change, v. 79, p. 176–192, doi:10.1016/j.gloplacha.2010.11.001.

- Bond, G.C., and Lotti, R., 1995, Iceberg Discharges into the North Atlantic on Millennial Time
- Scales During the Last Glaciation: Science, v. 267, p. 1005–1010,
- 208 doi:10.1126/science.267.5200.1005.
- Bond, G. et al., 1992, Evidence for massive discharges of icebergs into the North Atlantic ocean
- during the last glacial period: Nature, v. 360, p. 245–249.
- Briner, J.P., Goehring, B.M., Mangerud, J., and Svendsen, J.I., 2016, The deep accumulation of
- 212 10Be at Utsira, southwestern Norway: Implications for cosmogenic nuclide exposure dating
- in peripheral ice sheet landscapes: Geophysical Research Letters, v. 43, p. 9121–9129,
- 214 doi:10.1002/2016GL070100.
- 215 Briner, J.P., Gosse, J.C., and Bierman, P.R., 2006, Applications of cosmogenic nuclides to
- Laurentide Ice Sheet history and dynamics: Geological Society Special Paper, v. 415, p. 29–
- 217 41.
- 218 Briner, J.P., Lifton, N.A., Miller, G.H., Refsnider, K., Anderson, R., and Finkel, R., 2014, Using
- in situ cosmogenic 10Be, 14C, and 26Al to decipher the history of polythermal ice sheets on
- Baffin Island, Arctic Canada: Quaternary Geochronology, v. 19, p. 4–13,
- doi:10.1016/j.quageo.2012.11.005.
- Channell, J.E.T., Hodell, D.A., Romero, O., Hillaire-Marcel, C., de Vernal, A., Stoner, J.S.,
- Mazaud, A., and Röhl, U., 2012, A 750-kyr detrital-layer stratigraphy for the North Atlantic
- 224 (IODP Sites U1302-U1303, Orphan Knoll, Labrador Sea): Earth and Planetary Science
- 225 Letters, v. 317–318, p. 218–230, doi:10.1016/j.epsl.2011.11.029.
- 226 Corbett, L.B., Bierman, P.R., and Davis, P.T., 2016, Glacial history and landscape evolution of
- southern Cumberland Peninsula, Baffin Island, Canada, constrained by cosmogenic 10Be

- and 26Al: Bulletin of the Geological Society of America, v. 128, p. 1173–1192,
- doi:10.1130/B31402.1.
- Dalton, A.S. et al., 2020, An updated radiocarbon-based ice margin chronology for the last
- deglaciation of the North American Ice Sheet Complex: Quaternary Science Reviews, v.
- 232 234, p. 1–27, doi:10.1016/j.quascirev.2020.106223.
- Dalton, A.S., Stokes, C.R., and Batchelor, C.L., 2022, Evolution of the Laurentide and Innuitian
- ice sheets prior to the Last Glacial Maximum (115 ka to 25 ka): Earth-Science Reviews, v.
- 235 224, p. 103875, doi:10.1016/j.earscirev.2021.103875.
- Gosse, J.C., and Phillips, F.M., 2001, Terrestrial in situ cosmogenic nuclides: Theory and
- 237 application: Quaternary Science Reviews, v. 20, p. 1475–1560, doi:10.1016/S0277-
- 238 3791(00)00171-2.
- Grootes, Pieter Meiert; Stuiver, M., 1999, GISP2 Oxygen Isotope Data:,
- 240 doi:https://doi.org/10.1594/PANGAEA.56094.
- Grousset, F.E., Labeyrie, L., Sinko, J.A., Cremer, G., Duprat, J., Cortijo, E., and Huonll, S.,
- 242 1993, Patterns of Ice-Rafted Detritus in the Glacial North Atlantic (40-55 °N):
- Paleoceanography, American Geophysical Union, v. 8, p. 175–192.
- Gwiazda, R.H., Hemming, S.R., and Broecker, W.S., 1996, Provenance of icebergs during
- Heinrich Event 3 and the contrast to their sources during other Heinrich episodes:
- 246 Paleoceanography, v. 11, p. 371–378, doi:10.1029/96PA01022.
- Hemming, S.R., and Hajdas, I., 2003, Ice-rafted detritus evidence from 40Ar/39Ar ages of
- individual hornblende grains for evolution of the eastern margin of the Laurentide ice sheet
- since 43 14C ky: Quaternary International, v. 99–100, p. 29–43, doi:10.1016/S1040-
- 250 6182(02)00110-6.

- Hemming, S.R., 2004, Heinrich events: Massive late Pleistocene detritus layers of the North
- Atlantic and their global climate imprint: Reviews of Geophysics, v. 42,
- 253 doi:10.1029/2003RG000128.
- Hemming, S.R., Bond, G.C., Broecker, W.S., Sharp, W.D., and Klas-Mendelson, M., 2000,
- Evidence from 40Ar/39Ar ages of individual hornblende grains for varying Laurentide
- sources of iceberg discharges 22,000 to 10,500 yr B.P. Quaternary Research, v. 54, p. 372–
- 257 383, doi:10.1006/gres.2000.2181.
- Kleman, J., Jansson, K., de Angelis, H., Stroeven, A.P., Hättestrand, C., Alm, G., and Glasser,
- N., 2010, North American Ice Sheet build-up during the last glacial cycle, 115-21kyr:
- 260 Quaternary Science Reviews, v. 29, p. 2036–2051, doi:10.1016/j.quascirev.2010.04.021.
- Lambeck, K., Rouby, H., Purcell, A., Sun, Y., and Sambridge, M., 2014, Sea level and global ice
- volumes from the Last Glacial Maximum to the Holocene: Proceedings of the National
- Academy of Sciences of the United States of America, v. 111, p. 15296–15303,
- 264 doi:10.1073/pnas.1411762111.
- Lisiecki, L.E., and Raymo, M.E., 2005, A Pliocene-Pleistocene stack of 57 globally distributed
- benthic δ 18O records: Paleoceanography, v. 20, p. PA1003:1-17,
- 267 doi:10.1029/2004PA001071.
- 268 Mao, L., Piper, D.J.W., Saint-Ange, F., Andrews, J.T., and Kienast, M., 2014, Provenance of
- sediment in the Labrador Current: A record of hinterland glaciation over the past 125 ka:
- 270 Journal of Quaternary Science, v. 29, p. 650–660, doi:10.1002/jqs.2736.
- McManus, J.F., Oppo, D.W., and Cullen, J.L., 1999, A 0.5-Million-year record of millennial-
- scale climate variability in the North Atlantic: Science, v. 283, p. 971–975,
- 273 doi:10.1126/science.283.5404.971.

274	Miller, G.H., Briner, J.P., Lifton, N.A., and Finkel, R.C., 2006, Limited ice-sheet erosion and
275	complex exposure histories derived from in situ cosmogenic 10Be, 26Al, and 14C on Baffin
276	Island, Arctic Canada: Quaternary Geochronology, v. 1, p. 74-85,
277	doi:10.1016/j.quageo.2006.06.011.
278	Miller, G.H. et al., 2022, Last interglacial lake sediments preserved beneath Laurentide and
279	Greenland Ice sheets provide insights into Arctic climate amplification and constrain 130 ka
280	of ice-sheet history: Journal of Quaternary Science, v. 37, p. 979-1005,
281	doi:10.1002/jqs.3433.
282	Past Interglacials Working Group of PAGES, 2016, Interglacials of the last 800,000 years:
283	Reviews of Geophysics, v. 54, p. 162–219, doi:10.1029/88EO01108.
284	Pelletier, J.D., Broxton, P.D., Hazenberg, P., Zeng, X., Troch, P.A., Niu, G., Williams, Z.C.,
285	Brunke, M.A., and Gochis, D., 2016, Global 1-km Gridded Thickness of Soil, Regolith, and
286	Sedimentary Deposit Layers:, doi:http://dx.doi.org/10.3334/ORNLDAAC/1304.
287	Ruddiman, W.F., 1977, Late Quaternary deposition of ice-rafted sand in the subpolar North
288	Atlantic (lat 40° to 65°N): Bulletin of the Geological Society of America, v. 88, p. 1813-
289	1827, doi:10.1130/0016-7606(1977)88<1813:LQDOIS>2.0.CO;2.
290	Ullman, D.J., Carlson, A.E., Anslow, F.S., Legrande, A.N., and Licciardi, J.M., 2015, Laurentide
291	ice-sheet instability during the last deglaciation: Nature Geoscience, v. 8, p. 534-537,
292	doi:10.1038/ngeo2463.
293	
294	
295	
296	

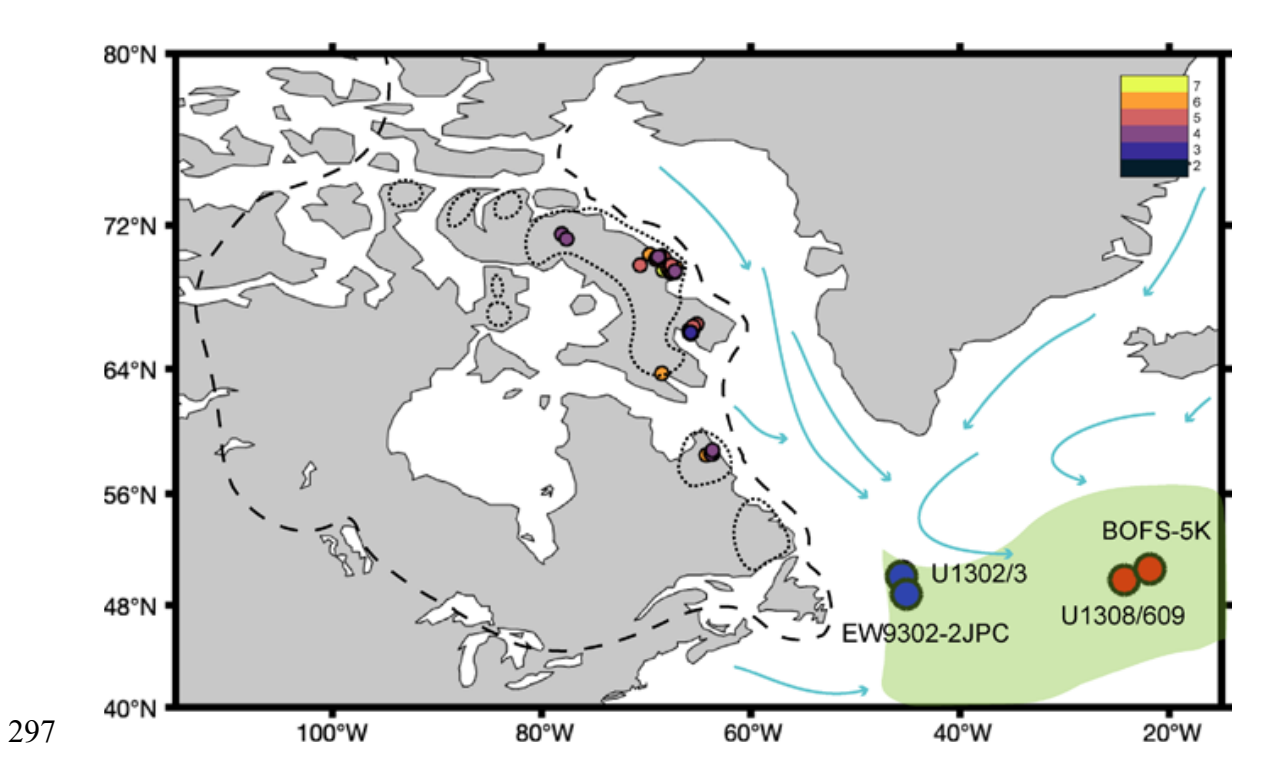


Figure 1. Cores analyzed in this study and ²⁶Al/¹⁰Be ratios in terrestrial bedrock from prior studies (Miller et al., 2006; Briner et al., 2006, 2014; Corbett et al., 2016). Also shown are the last glacial ice-rafted debris belt (light green), maximum and minimum estimates of

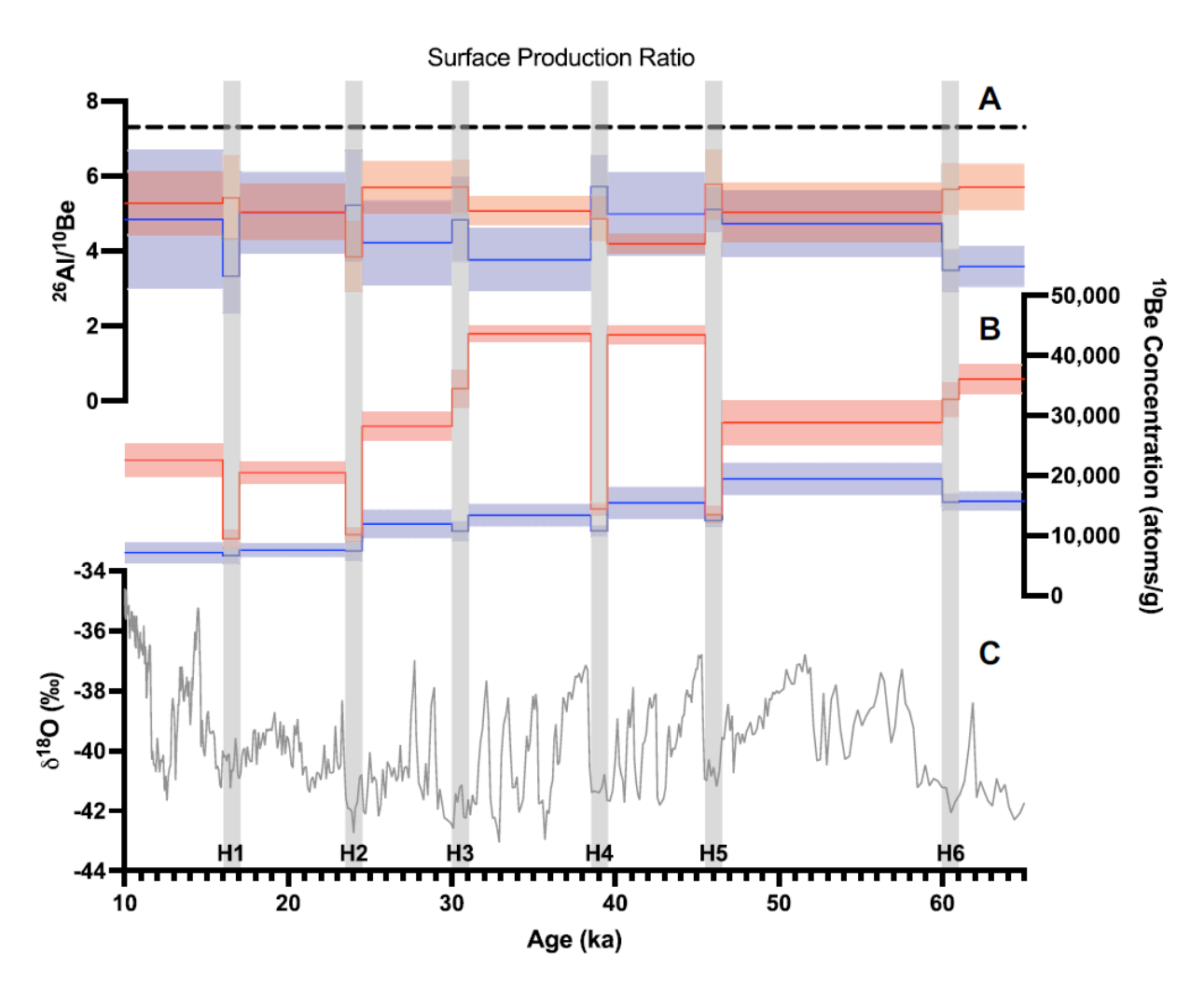


Figure 2. Measured (a) ²⁶Al/¹⁰Be ratios and (b) ¹⁰Be concentrations in ice-rafted debris from western (blue) and eastern (red) North Atlantic cores. Shading shows 1σ uncertainty. (c) GISP2

 δ^{18} O is shown as a proxy for Greenland temperature (Grootes and Stuiver, 1999). Heinrich layers are indicated by grey bars.



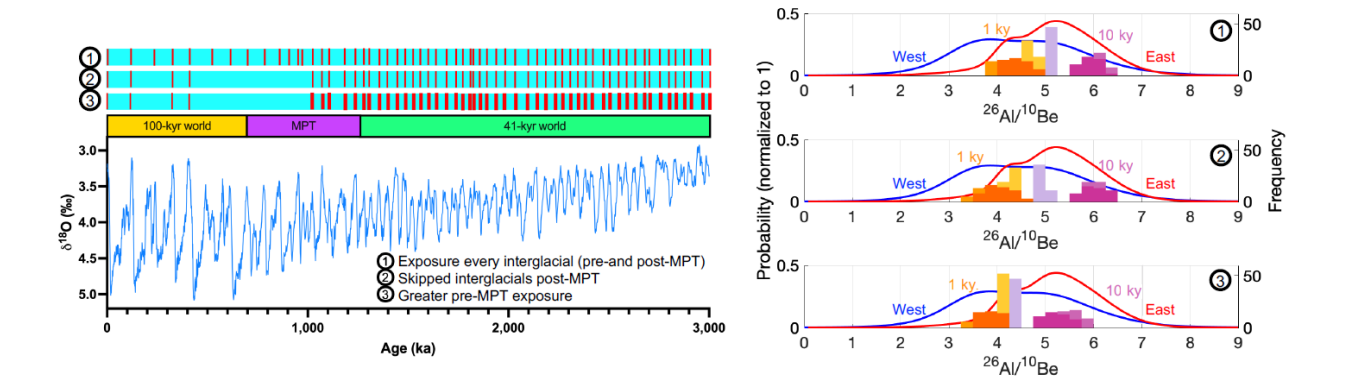


Figure 3. Modeled and measured ²⁶Al/¹⁰Be ratios in ice-rafted debris. (left) ¹⁰Be and ²⁶Al concentrations were simulated for three hypothetical ice cover scenarios, with interglacial exposures of 1- and 10-kyr lengths. Scenario 1 has exposure during every Pleistocene interglacial. Scenario 2 features exposure during every interglacial until 1 Ma, but only during select interglacials thereafter (MIS 1, 5e, 9, and 11). Scenario 3 is the same as scenario 2 but interglacial exposures are twice as long before 1 Ma as after (i.e., scenarios with 1- and 10-kyr exposures after 1 Ma have 2- and 20-kyr exposures before 1 Ma). (right) Histograms show simulated ²⁶Al/¹⁰Be ratios from 65-14 ka for 1-kyr (orange) and 10-kyr (purple) interglacial exposures using 1, 10, and 100 mm/kyr (from dark to light shading) subglacial erosion rates. Measured ²⁶Al/¹⁰Be ratios from the western (blue) and eastern (red) North Atlantic samples are shown as probability distribution functions. The LR04 δ¹⁸O stack is shown as a proxy for global ice volume.

325	¹ Supplemental Material. Additional information about materials and methods, forward modeling
326	simulations and data tables can be found therein. Please visit https://doi.org/10.1130/XXXX.
327	Additional information about materials and methods, forward modeling simulations and data
328	tables can be found therein. to access the supplemental material, and contact
329	editing@geosociety.org with any questions.